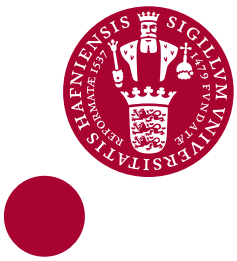

Large cryoconite aggregates on a Svalbard glacier support a diverse microbial community including ammonia-oxidizing archaea

Zarsky, Jakub D.; Stibal, Marek; Hodson, Andy; Sattler, Birgit; Schostag, Morten; Hansen, Lars H.; Jacobsen, Carsten Suhr; Psenner, Roland

Published in:
Environmental Research Letters

DOI:
10.1088/1748-9326/8/3/035044

Publication date:
2013

Document version
Publisher's PDF, also known as Version of record

Large cryoconite aggregates on a Svalbard glacier support a diverse microbial community including ammonia-oxidizing archaea

2013 Environ. Res. Lett. 8 035044

(http://iopscience.iop.org/1748-9326/8/3/035044)

OPEN ACCESS
IOP PUBLISHING ENVIRONMENTAL RESEARCH LETTERS
Environ. Res. Lett. **8** (2013) 035044 (11pp) doi:10.1088/1748-9326/8/3/035044

Large cryoconite aggregates on a Svalbard glacier support a diverse microbial community including ammonia-oxidizing archaea

Jakub D Zarsky[1], Marek Stibal[2,3], Andy Hodson[4,5], Birgit Sattler[1], Morten Schostag[2,3], Lars H Hansen[6], Carsten S Jacobsen[2,3] and Roland Psenner[1]

[1] Institute of Ecology, University of Innsbruck, Innsbruck, Austria
[2] Department of Geochemistry, Geological Survey of Denmark and Greenland (GEUS), Copenhagen, Denmark
[3] Center for Permafrost (CENPERM), University of Copenhagen, Copenhagen, Denmark
[4] Department of Geography, University of Sheffield, Sheffield, UK
[5] Department of Arctic Geology, The University Centre in Svalbard (UNIS), Longyearbyen, Norway
[6] Department of Biology, University of Copenhagen, Copenhagen, Denmark

E-mail: j.zarsky@gmail.com

Received 30 April 2013
Accepted for publication 9 August 2013
Published 11 September 2013
Online at stacks.iop.org/ERL/8/035044

Abstract
The aggregation of surface debris particles on melting glaciers into larger units (cryoconite) provides microenvironments for various microorganisms and metabolic processes. Here we investigate the microbial community on the surface of Aldegondabreen, a valley glacier in Svalbard which is supplied with carbon and nutrients from different sources across its surface, including colonies of seabirds. We used a combination of geochemical analysis (of surface debris, ice and meltwater), quantitative polymerase chain reactions (targeting the 16S ribosomal ribonucleic acid and *amoA* genes), pyrosequencing and multivariate statistical analysis to suggest possible factors driving the ecology of prokaryotic microbes on the surface of Aldegondabreen and their potential role in nitrogen cycling. The combination of high nutrient input with subsidy from the bird colonies, supraglacial meltwater flow and the presence of fine, clay-like particles supports the formation of centimetre-scale cryoconite aggregates in some areas of the glacier surface. We show that a diverse microbial community is present, dominated by the cyanobacteria, Proteobacteria, Bacteroidetes, and Actinobacteria, that are well-known in supraglacial environments. Importantly, ammonia-oxidizing archaea were detected in the aggregates for the first time on an Arctic glacier.

Keywords: glacier, cryoconite, microbial diversity, nitrogen, ammonia oxidation, Svalbard
S Online supplementary data available from stacks.iop.org/ERL/8/035044/mmedia

1. Introduction

Glaciers and ice sheets in the Arctic, including Svalbard, are melting at an accelerating rate (Kohler *et al* 2007, Pritchard *et al* 2009, Moholdt *et al* 2010, Nuth *et al* 2010, Gardner *et al* 2011), and receive considerable amounts of carbon (Slater *et al* 2002, Hansen and Nazarenko 2003, McConnell *et al* 2007) and nutrients (Hodson *et al* 2009, Samyn *et al* 2012, Björkman *et al* 2013) of various origin from the atmosphere and/or local sources. The liquid water produced during melting makes glacier surfaces habitable, and the debris and aerosols deposited on glaciers can serve

as a source of nutrients and viable microbial cells (Hodson *et al* 2008, Stibal *et al* 2012a). As a result, microorganisms grow and reproduce in the glacier surface debris, called 'cryoconite'. Active microbes associated with cryoconite produce cohesive compounds, called extracellular polymeric substances, which cause the aggregation of cryoconite on the ice surface (Takeuchi *et al* 2001, Hodson *et al* 2010, Langford *et al* 2010). Larger aggregates may be expected to have a longer residence time on the ice and thus enhance surface melting by their prolonged reduction of surface albedo (Bøggild *et al* 2010, Irvine-Fynn *et al* 2011). The large aggregates may also provide more microenvironments for a wider range of microorganisms and metabolic processes than smaller aggregates, since diffusion of oxygenated surface waters through them is less influential on the redox conditions found there (Hodson *et al* 2010, Langford *et al* 2010). These factors then enable cryoconite to contribute to ecological succession in the glacier forefield following the continued retreat of the glacier (Kaštovská *et al* 2007, Edwards *et al* 2013).

Most Arctic glaciers receive a substantial proportion of nitrogen by episodic atmospheric nitrogen enrichment from low-latitude sources (Kühnel *et al* 2012), and extreme nitrogen deposition events may far exceed inputs from snow accumulation and melt following the long winter accumulation period (Hodson *et al* 2009). Atmospheric deposition of nitrate and ammonium on Svalbard valley glaciers have increased 65% and 20% respectively since pre-industrial times, owing to anthropogenic pollution (Kekonen *et al* 2005). On the other hand, seabirds breeding on land may represent another source of nutrients for Arctic terrestrial ecosystems, including glaciers, due to guano deposition in the vicinity of their colonies (Stempniewicz 2005, Ellis *et al* 2006, Zwolicki *et al* 2013). Therefore, gradients of nutrient concentrations may be formed around bird colonies (Zmudczyńska *et al* 2008) in the Arctic that influence snow and ice ecology in a manner not unlike that already reported in the Antarctic (Hodson 2006). However, the relationship between terrestrial ecosystems in the predominantly ice-covered landscape of Svalbard and their adjacent marine ecosystems remains poorly understood. This uncertainty restricts our understanding of key biogeochemical cycles in this sensitive part of the Arctic.

Here we investigate the microbial community on the surface of Aldegondabreen, a small valley glacier in Svalbard, in order to better understand the potential for microbial utilization of nitrogen on the glacier surface. We present a combination of geochemical analysis of the surface debris, ice and meltwater, quantitative PCR targeting the 16S rRNA and *amoA* genes, pyrosequencing, and multivariate statistical analysis to better understand the likely functioning of this supraglacial ecosystem, with an emphasis on its potential to contribute to nitrogen cycling.

2. Methods

2.1. Field site and sampling

Aldegondabreen is a small (7.6 km^2) retreating valley glacier located in the Grønfjorden area of Spitsbergen, Svalbard, 77°58′N, 14°05′E (Navarro *et al* 2005). The debris on its surface (cryoconite) has three likely sources: first, debris avalanches from adjacent slopes with seabird breeding sites (mainly kittiwakes *Rissa tridactyla* and fulmars *Fulmarus glacialis* on the northern slope and little auks *Alle alle* on the southern slopes), second, airborne dust originating from deglaciated areas (Bullard 2013), including adjacent slopes, and third, a coal power plant in the mining settlement of Barentsburg acting as a rich local source of air borne black carbon. Significant local input of debris into the supraglacial environment in combination with variable slope of the ablation zone makes this locality an interesting case of a supraglacial ecosystem with a high spatial variation of biogeochemical characteristics on a small area (figure 1). This is supported by the results of Langford *et al* (2011) who found considerable mineralogical and geochemical diversity in the cryoconite aggregates from Aldegondabreen.

Samples of cryoconite and supraglacial meltwater, and shallow ice cores, were collected at ten sites on the surface of Aldegondabreen (figure 1) between 22 and 24 July 2009. The sampling sites were categorized according to the slope of transects and their hydrological connection to the mountain sides on both edges of the glacier or the up-glacier snow pack. Bulk cryoconite sediment was collected (regardless of its structure) using a sterile plastic syringe and placed in a sterile WhirlPak bag (Nasco, Fort Atkinson, WI, USA). The samples were kept on ice in the dark (cooled with whirlpak bags filled with glacial ice in an aluminum zarges box) until 26 July when they were frozen to −20 °C at the laboratory at UNIS, ca 70 km away (5 h by boat). Ice cores (1 m) were taken using a hand-driven Kovacs Mark III ice corer (Kovacs Enterprises, Lebanon, NH, USA) after removing the surface layer of 5–10 cm of sediment-rich ice with an ice axe to separate the chemical signal of glacial ice from cryoconite and melted snow. Due to the fragile nature of the ice cores two sterile 2 l WhirlPak bags were filled with ice from the bottom part of the core. The remaining upper part of the ice cores was discarded. The ice samples were then melted in the bags in the dark and filtered using a Millipore filtering device with a vacuum hand pump and polycarbonate filters of 47 mm diameter and 0.22 μm pore size (Millipore, Billerica, MA, USA). Samples of supraglacial stream water were collected directly into sterile 2 l WhirlPak bags and immediately filtered as above. The filtration device was pre-rinsed with sample and filtrate twice before retention of the sample as there was no access to deionized water. The filtered water samples were then separated into sterile 100 ml WhirlPak bags and kept in the cold and dark until 26 July when they were frozen to −20 °C. All samples were then transported frozen in an insulated box to Innsbruck. Sterile powder-free gloves were used for sample collection and handling.

2.2. Chemical analysis

Total carbon (TC) and nitrogen (TN) in the cryoconite sediment samples were analysed using a Flash EA 1112 analyzer (Thermo Electron Corporation, Delft, the

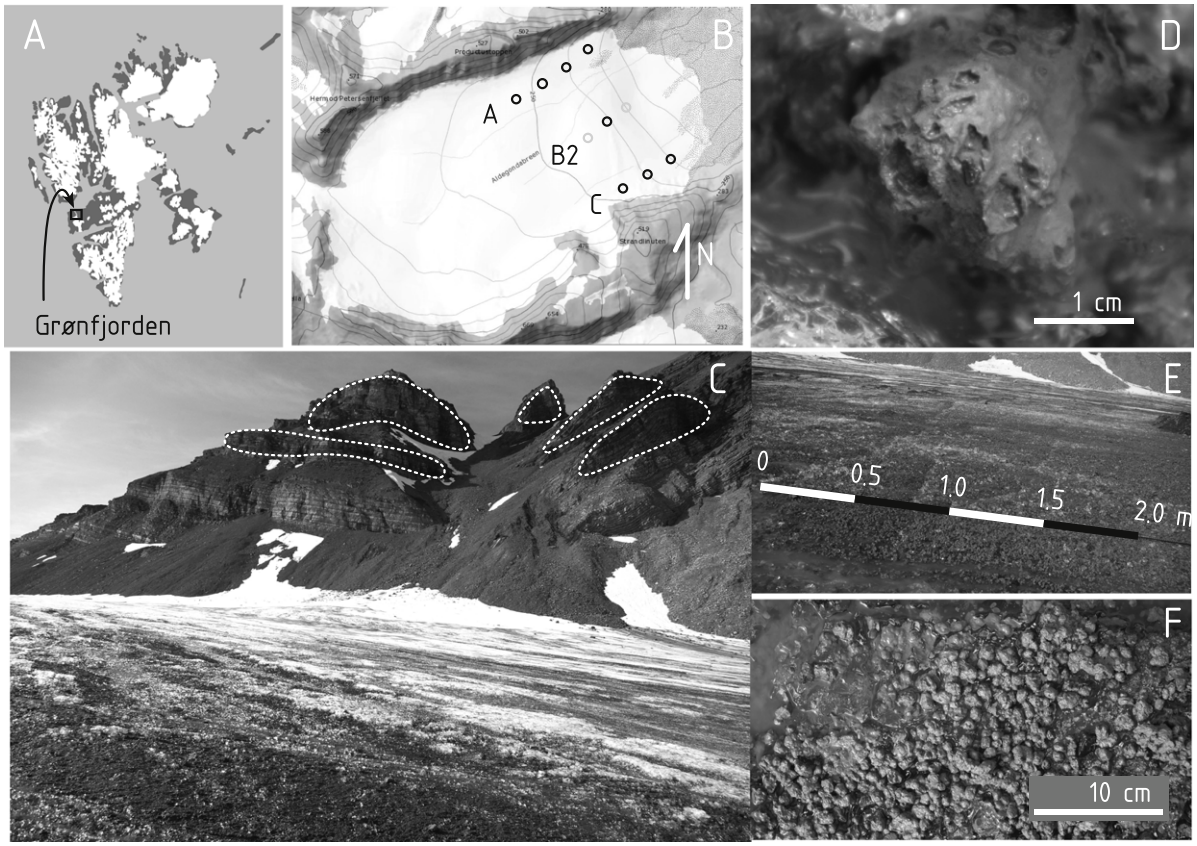

Figure 1. (A) Aldegondabreen in Grønfjorden, the study site in Svalbard. (B) Location of the sampling sites on the surface of Aldegondabreen. Transects (A)–(B) are numbered from the lowest point upstream. In transect (B) only the point B2 was analysed. (C) Northern margin of Aldegondabreen with sampling points A3 and A4 as seen from point A2 with marked areas of bird nesting activity and occurrence of large cryoconite granules. White circles indicate the area in the slopes of Productustoppen (527 m) with nesting seabirds. (D) Large cryoconite aggregate in detail with visible cyanobacterial mat on its surface. (E) View on the glacier surface at transect (A). The scale was derived from an 3 m long avalanche probe with cm scale. The probe is visible in the lower right part of the shot. The cryoconite aggregates cover the surface without producing deep melt ponds due to prevailing effect of conductive heat flux. (F) Large cryoconite sediment aggregates at point A2.

Netherlands) in the NC Soils configuration. All samples were dried at 105 °C for 24 h prior to analysis. For the determination of TP (total phosphorus), pre-weighted sediment samples were suspended in 100 ml of deionized water and 1 ml 96% H_2SO_4 was added. The samples were then stored in a drying cabinet for 12 h at 160 °C. Approximately 93 ml of distilled water was added and the mixture was cooled down to room temperature. Afterwards 6 ml of 10% ascorbic acid and 6 ml 20% NaOH was added, and the solution was neutralized with Vogler solution (Vogler 1966). The absorbance of the samples at 885 nm was measured using a U-2000 spectrophotometer (Hitachi, Tokyo, Japan). The detection limit was 0.9 μg l^{-1}. Dissolved organic carbon (DOC) and total dissolved nitrogen (TDN) were determined using a TOC-V_{CPH}/TNM-1 analyser (Shimadzu, Kyoto, Japan). DOC was measured as the carbon remaining after acidification with 2 M HCl. Detection limit for both DOC and TDN is 4 μg l^{-1}. Ion chromatography (Dionex ICS-1000, Dionex, Camberley, UK) was used for the determination of ion concentrations (NO_3^-, NH_4^+). The detection limits were 5.0 μg l^{-1} for both NO_3^- and NH_4^+. Due to logistical constraints, only one sample per site could be transported and analysed.

2.3. Particle size and size of aggregates

Particle size was measured using high-resolution laser diffractometry particle size analysis with a Mastersizer 2000 (Malvern Instruments, Malvern, UK). Dried cryoconite sediment (105 °C for 24 h) was suspended in deionized water up to the lower range of optimal obscuration level. The particle size range of this method is 0.02–2000 μm. Samples were sonicated using a built-in sonicator in order to break apart particle aggregates. To assist the dispersion of particles and to avoid their aggregation after sonication, sodium hexametaphosphate ($NaPO_3$) was added to a concentration of 5.5 g l^{-1} (Sperazza *et al* 2004). Preliminary measurements showed a minimal change in particle size distribution after sonication longer than 120 s and, therefore, a sonication time of 120 s was used for all samples. Fineness of sediment was calculated from the particle size distribution as surface area per gram of dry sediment, assuming the prevailing material of the particles being $CaCO_3$ for density (2.71 g cm^{-3})

Table 1. Primer sets used for qPCR of 16S rRNA and *amoA* genes from the cryoconite samples.

Primer	Sequence (5′ → 3′)	Annealing T	Organism	Reference
		16S rRNA		
341F 518R	CCT ACG GGA GGC AGC AG ATT ACC GCG GCT GCT GG	60 °C	Bacteria	Muyzer *et al* (1993)
		amoA		
amoA-1F amoA-2R	GGG GTT TCT ACT GGT GGT CCC CTC KGS AAA GCC TTC TTC	58 °C	Ammonia-oxidizing bacteria	Rotthauwe *et al* (1997)
19F A616r48×	GGW GTK CCR GGR ACW GCM AC GCC ATC CAB CKR TAN GTC CA	55 °C	Ammonia-oxidizing archaea	Leininger *et al* (2006) Schauss *et al* (2009)

estimation and a spherical particle shape, using the Malvern Mastersizer 2000 software. The approach of using sediment surface area per dry weight (fineness) was chosen as a proxy for potential 'microbial landscape' (Battin *et al* 2007).

Aggregate size (diameter of cryoconite macroscopic aggregates, figures 1(d) and (f)) was measured from photographs using the image analysis software ImageJ 1.43u. Images were photographed with a scale in the field and for each aggregate two Feret diameters were measured: first along the longest visible dimension of the aggregate and second perpendicular to it. The mean of both measurements was used to represent aggregate diameter. Only undisturbed aggregates were measured, excluding clusters of aggregates or fragments.

2.4. Microbiological analysis

Extraction of DNA from the cryoconite samples was performed using the PowerLyzer PowerSoil DNA Isolation Kit (MO BIO Laboratories, Carlsbad, CA, USA) according to the manufacturer's instructions. Between 0.2 and 0.9 g (wet weight) of sediment was used for each extraction, and a blank containing no sediment was extracted in parallel. The quantity of total bacteria and ammonia-oxidizing bacteria and archaea was determined by quantitative PCR (qPCR) with primers targeting the bacterial 16S rRNA gene and the bacteria- and archaea-specific *amoA* genes encoding the active site of ammonia monooxygenase (table 1). The qPCR was set up under DNA free conditions in a pressurized clean-lab that has an HEPA filtered air inlet and is UV-irradiation sterilized for 3 h on a daily basis. The setup was as follows: 20 μl reactions containing 10 μl of SYBR Premix Ex Taq II (TaKaRa, Kyoto, Japan), 0.8 μl of the primers (final concentration 0.4 μM) and 1 μl of template DNA. The reaction was then carried out on a CFX96 Touch qPCR system (Bio–Rad, Hercules, CA, USA) equipped with high-resolution melt (HRM) analysis. HRM analysis is a quantitative analysis of the melt curves of product DNA fragments, allowing for the identification of small variations in nucleic acid sequences by the controlled melting of double-stranded PCR amplicons and clustering of samples according to their similarity (Garritano *et al* 2009). The cycle program was 95 °C for 1 min followed by 50 cycles of 95 °C for 30 s, 30 s at the respective annealing temperature (table 1), and 72 °C for 30 s. The reaction was completed by a final 72 °C elongation step for 6 min and followed by HRM analysis in 0.1 °C increments from 72 to 95 °C. All qPCR reactions were performed in triplicate. Standards of the bacterial 16S rRNA gene and bacterial and archaeal *amoA* were prepared as dilution series from cultures of *Escherichia coli*, *Nitrosomonas europaea* ATCC19718 derived lux-marker strain (Iizumi *et al* 1998), and fosmid clone 54d9 (Treusch *et al* 2005), respectively, with known cell abundances. The gene copy numbers in the highest standards were 1.66×10^9 μl^{-1} for 16S rRNA, 3×10^7 for bacterial *amoA*, and 3×10^8 for archaeal *amoA*.

The diversity of prokaryotic microorganisms in the samples was determined by pyrosequencing. One sample from each cluster showed in the HRM analysis was selected for sequencing. Amplicons (466 bp) flanking the V3 and V4 regions of the 16S rRNA gene were amplified using the primers 341F (5′-CCTAYGGGRBGCASCAG-3′) and 806R (5′-GGACTACNNGGGTATCTAAT-3′) followed by a second round of PCR where primers with adapters and 10 bp tags were used (Hansen *et al* 2012). PCR amplification was performed using 1× AccuPrime buffer II which includes 0.2 mM dNTP's, 0.75 U AccuPrime Taq DNA Polymerase High fidelity (Invitrogen, Carlsbad, CA, USA), 0.5 μM of each of the primers, and 1 μl of DNA sample to a total of 25 μl reaction. PCR was performed with a DNA Engine Dyad Peltier Thermal Cycler (MJ Research, Massachusetts, USA), using the following cycle conditions: 94 °C for 2 min, followed by 30 cycles of denaturation at 94 °C for 20 s, annealing at 56 °C for 30 s and elongation at 68 °C for 40 s, and then a final elongation step at 72 °C for 5 min. The conditions of the second PCR were as the first PCR, except that the number of cycles was reduced to 15 cycles. The PCR products were run on a gel and the appropriate fragments were cut and purified using the Montage DNA Gel Extraction kit (Millipore, Bedford, MA, USA). The amplified fragments with adapters and tags were quantified using a Qubit fluorometer (Invitrogen, Carlsbad, CA, USA) and mixed in approximately equal concentrations (1×10^7 copies μl^{-1}) to ensure equal representation of each sample. Samples were run on one of a two-region 454 sequencing run was performed on a GS FLX Titanium Pico TiterPlate using a GS FLX Titanium Sequencing Kit XLR70 according to the manufacturer's instructions (Roche Diagnostics, Indianapolis, IN, USA).

Table 2. Geographical parameters of the sampling sites on Aldegondabreen.

Site	Hydrological connection to mountain side	Altitude (m a.s.l.)	Slope (deg)	Sediment fineness ($m^2\ g^{-1}$)
A1	Connected	165	6.8	0.705
A2	Connected	200	6.8	0.761
A3	Connected	240	6.8	0.751
A4	Connected	280	6.8	0.633
B2	Isolated	170	6.6	0.505
C1	Connected	150	9.3	0.526
C2	Connected	200	9.3	0.433
C3	Connected	250	9.3	0.473

The obtained sequencing data were analysed with the QIIME Pipeline (Caporaso *et al* 2010). Sequences were filtered out if they did not fulfil the following criteria: perfect match to the sequence primer of the 16S rRNA gene; length between 200 and 1000 bp; maximum 6 ambiguous bases; minimum score of 50 in the quality score window; no homopolymer longer than 6 bp; maximum number of errors in barcode 1.5. After filtering the sequences were denoised using the default option in QIIME and clustered into Operational Taxonomic Units (OTUs) using Uclust (Edgar 2010) with a 97% sequence similarity. The first cluster seed in the OTU step was used as a representative sequence for each OTU. Representative sequences were then used for taxonomic classification using RDP classifier (Wang *et al* 2007) with a confidence threshold of 0.8 against the Greengene core set (DeSantis *et al* 2006). Phylogenetic analysis was performed on selected sequences. They were aligned together with 16S rRNA gene sequences of closest relatives identified with BLAST at the National Center for Biotechnology Information using MUSCLE (Edgar 2004), and edited manually in JalView (Waterhouse *et al* 2009). Analysis was restricted to nucleotide positions that were unambiguously aligned in all sequences. The phylogenetic tree was constructed using the maximum likelihood method using MEGA version 5 (Tamura *et al* 2011). Bootstrap analysis (1000 replications) was used to provide confidence estimates for phylogenetic tree topologies.

16S rRNA gene sequences obtained in the pyrosequencing analysis have been deposited in the Sequence Read Archive (SRA) at the National Center for Biotechnology Information (NCBI) under accession number SRR896648. Interactive charts visualising pyrosequencing data are available as supplementary material (stacks.iop.org/ERL/8/035044/mmedia).

2.5. Statistical analysis

Multivariate statistical analysis was used in order to explain the variation in the data and to test the significance of environmental effects on the chemistry and the abundance of total and ammonia-oxidizing microbes. All the quantitative data except altitude were $\ln(x + 1)$ transformed prior to analysis. The hydrological connection to the mountain sides was used as a categorical variable, based upon direct field observations. All data were standardized and centred. Detrended canonical correspondence analysis (DCCA) was used to determine the length of the gradient along the first ordination axis in order to select the appropriate method for ordination of the data. Redundancy analysis (RDA) was then used in order to assess the relationships between known environmental variables and variation in the multivariate data. 999 Monte Carlo permutations in the unrestricted mode, and manual forward selection, were used for the RDA. The results of the RDA were summarized using biplot or triplot diagrams. The relative length and position of arrows in the diagrams show the extent and direction of response of the selected dependent variables to the environmental factors. All the analyses were performed in the multivariate data analysis software Canoco 5 (ter Braak and Šmilauer 2012).

3. Results

Unexpected complications with molecular analysis required many repeat trials. Since logistical restrictions imposed constraints on the transport of material, these complications meant not all samples were available in a sufficient quantity and so we are only able to present a large subset of the original samples (see figure 1(B)). Table 2 shows the physical characteristics of the sampling sites. The altitude of the sites ranged from 150 m (lower end of transect C) to 280 m a.s.l. (upper end of transect A). The slope of the glacier surface declined from south to north, being steepest (>9°) on transect C. Point B2 was fed solely from streams originating in melting ice and/or snow with no hydrological connection to the slopes above the glacier, whereas the other points (A and C transects) were hydrologically connected to adjacent mountain slopes. Sediment fineness of the samples ranged from 0.43 $m^2\ g^{-1}$ to a maximum of 0.76 $m^2\ g^{-1}$ ($0.60 \pm 0.13\ m^2\ g^{-1}$). The cryoconite aggregate diameter at transect A ranged from 0.42 to 3.1 cm (1.1 ± 0.35 cm, $n = 350$). The aggregate size distribution is shown in figure 2. No large aggregates with distinct coating of cyanobacterial mats were found in parts of the glacier other than transect A, although small aggregates of millimetre size and irregular fragments of larger aggregates were ubiquitous.

Table 3 shows the concentrations of sediment-bound and dissolved nutrients in the samples from the surface of Aldegondabreen. The concentrations of DOC ranged from 0.40 to 2.0 $mg\ l^{-1}$ ($0.96 \pm 0.50\ mg\ l^{-1}$; $n = 8$) in supraglacial meltwater, and from 0.34 to 1.4 $mg\ l^{-1}$ ($0.60 \pm 0.34\ mg\ l^{-1}$) in surface ice. TDN was between 34 and 180 $\mu g\ l^{-1}$ ($110 \pm 50\ \mu g\ l^{-1}$) in supraglacial meltwater and between 16 and 61 $\mu g\ l^{-1}$ ($38 \pm 16\ mg\ l^{-1}$) in surface ice. The concentration

Table 3. Nutrient concentrations in cryoconite sediment, supraglacial meltwater, and surface ice on Aldegondabreen. TC (total carbon), TN (total nitrogen), TP (total phosphorus) in mg g^{-1} (mean ± sd, $n = 3$); DOC (dissolved organic carbon) in mg l^{-1}, TDN (total dissolved nitrogen), NO_3^-, NH_4^+ in $\mu g\ l^{-1}$. b.d. below detection limit; n.d. not determined.

	Sediment			Supraglacial meltwater				Surface ice			
Site	TC	TN	TP	DOC	TDN	NO_3^-	NH_4^+	DOC	TDN	NO_3^-	NH_4^+
A1	25 ± 0.87	2.4 ± 0.04	0.78 ± 0.029	0.87	100	b.d.	b.d.	0.49	32	b.d.	b.d.
A2	26 ± 0.40	2.7 ± 0.10	0.75 ± 0.066	0.79	12	11	12	1.40	48	b.d.	b.d.
A3	26 ± 3.6	2.2 ± 0.16	0.72 ± 0.004	0.53	53	16	5.0	0.41	49	b.d.	8.0
A4	23 ± 0.60	1.9 ± 0.07	0.70 ± 0.045	1.29	160	24	10	0.63	61	b.d.	11
B2	57 ± 2.1	2.5 ± 0.20	0.77 ± 0.010	1.00	120	7.0	16	0.34	18	7.0	7.0
C1	46 ± 2.5	2.0 ± 0.08	0.69 ± 0.023	1.99	180	7.0	27	0.50	39	n.d.	n.d.
C2	17 ± 0.67	1.2 ± 0.04	0.69 ± 0.017	0.40	34	b.d.	11	0.60	43	b.d.	13
C3	21 ± 1.7	1.5 ± 0.10	0.69 ± 0.009	0.79	120	7.0	30	0.40	16	7.0	8.0

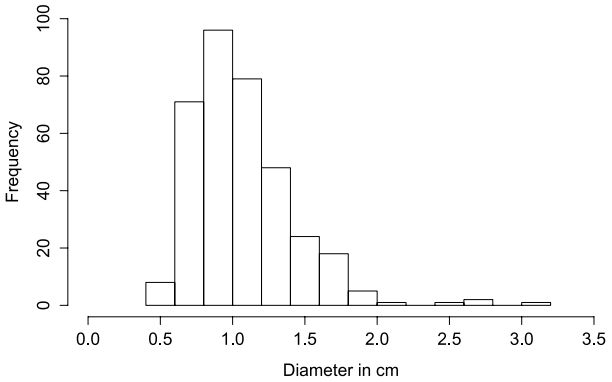

Figure 2. Histogram of aggregate diameters at transect A, site A2.

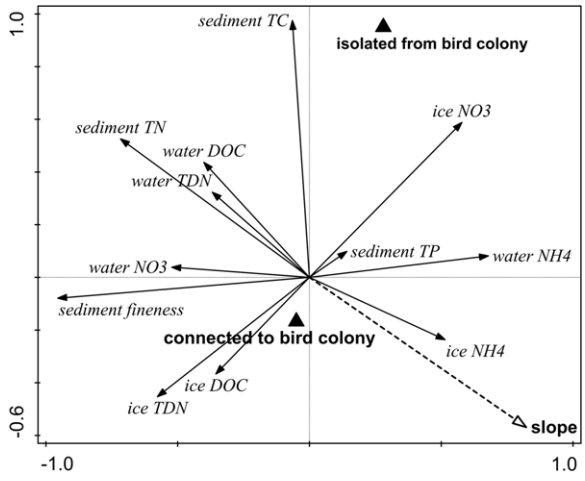

Figure 3. RDA biplot visualizing the effects of physical environmental variables (dashed arrows for quantitative and filled triangles for categories) on the chemistry (solid arrows) of cryoconite holes on Aldegondabreen. Only significant factors ($p < 0.01$) are shown.

of NO_3^- in supraglacial meltwater ranged from values below detection limit (points A1 and C1) to 24.0 $\mu g\ l^{-1}$ at point A4. The concentrations of NO_3^- in surface ice were close to (7 $\mu g\ l^{-1}$ at B2 and C3) or below detection limit. NH_4^+ ranged from below detection limit to 30 $\mu g\ l^{-1}$ with a mean of 14.3 (±9.7) $\mu g\ l^{-1}$ in meltwater, and from 5 to 13 $\mu g\ l^{-1}$ (7.7 ± 3.5 $\mu g\ l^{-1}$) in surface ice (table 3). The DOC:TDN ratio in supraglacial meltwater ranged from 7.4 to 14 (10 ± 2.3; $n = 8$) and from 10 to 34 (19 ± 8.4) in surface ice. The mean sediment-bound C:N molar ratio in the samples was 17 ± 6.0 ($n = 24$), with a minimum of 11 ± 0.40 at point A2 and a maximum of 27 at B2 and C1. The mean C:P molar ratio was 108 ± 46 with two outlier maxima of 190 ± 9.6 and 170 ± 6.1 at B1 and C1, respectively. Mean N:P ranged from 3.9 ± 0.64 (C2) to 8.0 ± 0.38 (A2), with an overall average of 6.2 ± 1.3. Figure 3 shows the results of an RDA analysing the variation in the chemistry data using the hydrological connection to a bird colony (connected versus isolated), altitude, and slope. The analysis explained 48.6% of the total variation in the data, with slope (26.1%, $p = 0.001$) and bird colony connection (22.4% of variation, $p = 0.001$) as significant factors.

Table 4. Abundances of the 16S rRNA gene and bacterial and archaeal *amoA* genes (gene copies g^{-1}) in cryoconite on Aldegondabreen (mean ± sd; $n = 3$). b.d. below detection limit.

Site	16S rRNA ($\times 10^7$)	Bacterial *amoA* ($\times 10^4$)	Archaeal *amoA* ($\times 10^4$)
A1	320 ± 0.76	0.28 ± 0.11	26 ± 1.2
A2	120 ± 1.8	0.011 ± 0.02	16 ± 5.3
A3	230 ± 59	1.4 ± 0.10	22 ± 11
A4	230 ± 15	0.29 ± 0.074	25 ± 0.26
B2	4.0 ± 0.92	b.d.	b.d.
C1	140 ± 16	b.d.	b.d.
C2	180 ± 1.1	b.d.	b.d.
C3	30 ± 2.0	b.d.	b.d.

Table 4 shows the results of the qPCR analysis of the 16S rRNA and *amoA* genes in the cryoconite samples. The abundance of the 16S rRNA gene was lowest (4.0×10^7 gene copies per g of wet sediment) at point B2 and highest on transect A ($1.2–3.2 \times 10^9$ g^{-1}). The high precision melt curve analysis coupled to the qPCR with 16S rRNA primers clustered the samples according to their similarity into four groups (A1–A2; A3–A4; B2; C1–3; data not shown). One representative was selected from each group (A1, A4, B2 and C2) for subsequent pyrosequencing. The *amoA* genes were only detected in samples from transect A (table 4). The abundance of bacterial *amoA* in the A samples was between ∼100 and 14 000 gene copies per g, while that of the archaeal *amoA* was one to two orders of magnitude higher, ranging from 16 to 26 $\times$ 10^4 g^{-1}. Figure 4 shows the results of an RDA analysis in which the variation in the qPCR data

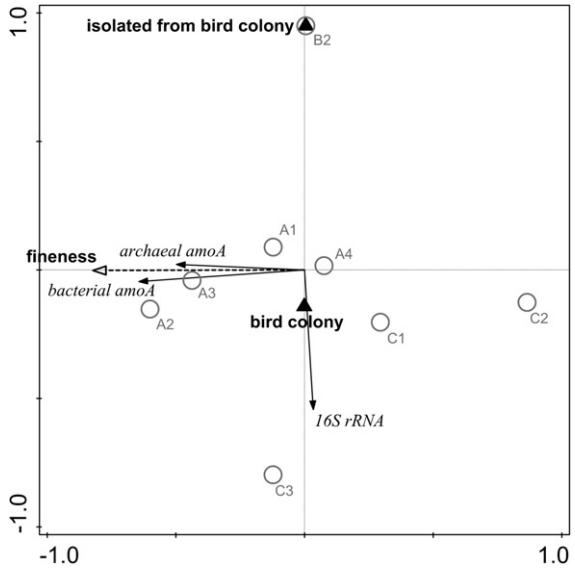

Figure 4. RDA triplot showing the effects of environmental variables (dashed arrows for quantitative and filled triangles for categories) on the abundance of 16S rRNA and *amoA* genes (solid arrows) in cryoconite holes on Aldegondabreen. Sites are marked by empty grey circles. Only significant factors ($p < 0.01$) are shown.

Table 5. Sequencing depth and diversity and dominance indices for the selected samples of cryoconite from Aldegondabreen.

Site	Sequences per sample
A1	58 171
A4	33 334
B2	357
C2	52 796

(both 16S rRNA and *amoA*) was explained using physical (mountain slope connection, slope, sediment fineness) and chemical (sediment TC, TN, TP, water DOC, NH_4^+ and NO_3^-) data as predictors. The weight of sediment used for DNA extraction was used as a covariate. The analysis explained 57.8% of the total variation in the qPCR data, with sediment fineness explaining 39.9% ($p = 0.001$) and mountain slope connection 17.9% ($p = 0.002$).

Table 5 shows the results of the pyrosequencing analysis of the selected samples. The average sequence length after quality check was 461 bp (ranging between 186 and 522 bp). Between ~33 000 and 58 000 sequences were obtained for all samples except B2, for which only 357 sequences were generated. The highest diversity as expressed by the Shannon index was found in sample A4, whereas sample B2 showed the highest dominance (Berger–Parker index). The prokaryotic diversity in the samples on the phylum level is shown in figure 5. Cyanobacteria were the dominant group in all samples except A4, accounting for over 60% of the community in sample A1. Proteobacteria (14–33%), Bacteroidetes (2.0–23%) and Actinobacteria (1.4–34%) were also present in high numbers in all the samples. The dominant sequences in A1 were filamentous cyanobacteria of the genera *Microcoleus* (17%) and *Phormidium* (11%) and a member of Bacteroidetes related to *Sphingobacteria* (5%).

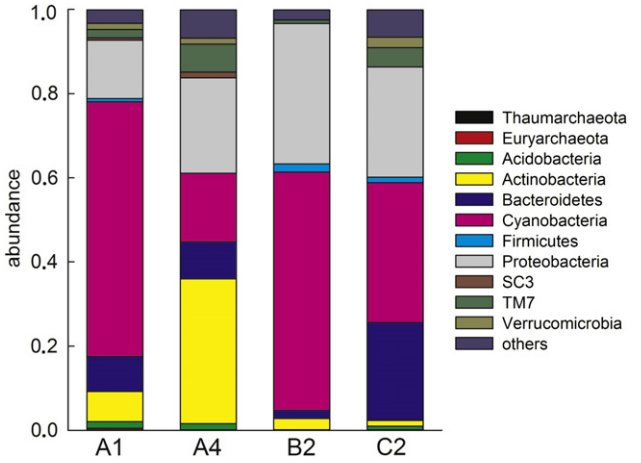

Figure 5. Diversity of prokaryotic phyla in the samples selected for pyrosequencing, expressed as a proportion of the total sequences. Eubacterial phyla accounting for less than 0.5% of the sequences were pooled into 'others'.

Sequences related to the ammonia-oxidizing *Nitrososphaera* (Thaumarchaeota) were detected in sample A1, accounting for 0.11% of the community (figures 5 and 6). The dominant sequences in A4 were members of Actinobacteria (*Knoellia* and another related sequence, accounting for 2% and 13%, respectively), and sequences related to *Sphingomonas* and *Rhodobacter* (Proteobacteria; 5.0% and 4.0% respectively). Sample B2 was dominated (55%) by a sequence related to a chloroplast. Sample C2 was dominated by sequences related to *Sphingobacteria* (Bacteroidetes; 18%) and filamentous cyanobacteria (i.e. *Phormidium*, 10%). No archaea were detected in A4, B2 or C2. No known ammonia-oxidizing bacteria were detected in any of the samples.

4. Discussion

Aldegondabreen is an example of a small Arctic valley glacier with marked spatial variations in the physical and chemical environments across its surface. The amount of debris can be significant on the surface of Aldegondabreen and exceed 4 kg m^{-2}. Due to the vicinity of the mining settlement of Barentsburg, black carbon (BC) can represent an important contribution to this debris. However, our field reconnaissance and statistical analyses (table 3) showed lateral inputs of material at different locations on the glacier and their redistribution by slope avalanching and runoff were particularly significant. However, the missing data points from the centre of the glacier undermine the statistical analysis to some extent, and so it should also be noted that Langford *et al* (2011) found clear differences between the mineral debris in the centre of the glacier (principally wind input) and at its sides (mainly avalanche input) using geochemical analysis. Langford *et al* (2011) also found significant spatial variability in organic matter composition on the glacier surface, with cryoconite near to the centre dominated by carbohydrate-rich organic matter and associated humification products, whilst cryoconite near to the glacier edge contained both a lesser quantity and a less diverse composition of organic matter.

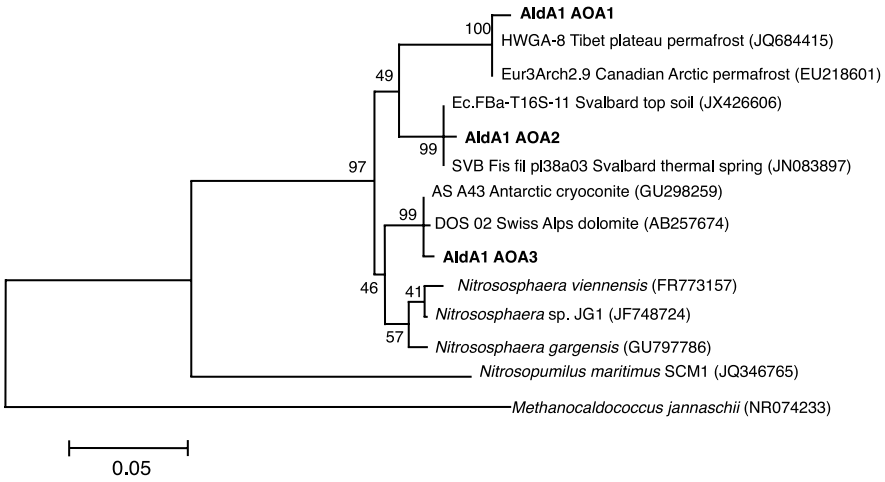

Figure 6. Phylogenetic analysis of the nitrososphaeraceae sequences identified in the 454 pyrosequencing dataset from cryoconite sample A1 (in bold). The maximum likelihood tree was constructed based on 406-base-pair-long 16S rRNA sequences and rooted with *Methanocaldococcus jannaschii*.

This is consistent with our data showing the highest content of OC in cryoconite at point B2 in the centre of the glacier (table 3) and the differences therefore most likely result from the avalanching of freshly eroded rock at the glacier margins.

The size of the Aldegondabreen cryoconite aggregates (figures 1 and 2) is typically far in excess of those found on other glaciers and offers rather different habitat to the mm-scale aggregates described elsewhere (Hodson *et al* 2010, Takeuchi *et al* 2010). We therefore propose that the combination of a relatively gentle slope of the glacier surface, fine sediment derived from local shales, and input of nutrients associated both with the avalanche debris and atmospheric deposition collectively enable the development of large cryoconite aggregates that support a distinct microbial community. The microbes then further facilitate the growth of the aggregates through production of extracellular polymeric substances that have cohesive properties (Hodson *et al* 2010, Langford *et al* 2010).

The total microbial abundance in cryoconite on Aldegondabreen, determined as the abundance of the 16S rRNA genes, is consistent with previous data from other Svalbard glaciers based on microscopy counts (Stibal *et al* 2008a, Anesio *et al* 2010, Langford *et al* 2010). The structure of the microbial community is also similar to that of other Svalbard sites (Edwards *et al* 2011, Cameron *et al* 2012a) and dominated by photoautotrophic cyanobacteria and mostly heterotrophic Proteobacteria, Bacteroidetes, and Actinobacteria (figure 5). The difference in cyanobacterial abundance between the samples may be attributed to the fact that chloroplasts are also identified as cyanobacteria, and that a significant amount of plant residue from nearby tundra can be deposited on the glacier surface by aeolian transport. We also suggest that the high dominance of a chloroplast sequence in sample B2 was caused by the presence of chloroplast-containing plant tissue in the sample; this may also have caused a lower efficiency of molecular analysis and led to the low number of sequences retrieved from the pyrosequencing analysis (table 5).

The slope of the glacier surface is assumed to affect the development of cryoconite aggregates most via the erosive action of meltwater, which is supported by the fact that transect A contained the largest, well-developed cryoconite aggregates (figure 1(d)) even though both edges of the glacier were influenced by inputs from the mountain sides. Although the difference in slope between the side transects (A versus C) was relatively small (ca 2.5°), our RDA analysis showed a significant effect of it on the concentrations of DOC and both sediment-bound and dissolved total nitrogen (figure 3). Again, while the statistical analysis is undermined by the missing data from transect B, the importance of flowing water has been noticed before on Arctic glaciers (Edwards *et al* 2011, Stibal *et al* 2012b). In fact even smaller differences in slope were shown to control nutrient concentrations and microbial abundance and activity on the surface of the Greenland Ice Sheet (Stibal *et al* 2012b).

Sediment fineness, being a measure of particle surface area per sediment dry weight, is assumed to affect the formation of cryoconite aggregates simply due to the surface area available for adhesion of microbial cells, their products, or other sticky substances. This is consistent with the presence of large granules only on transect A which contained the finest sediment (table 2). The size distribution of aggregates measured at transect A shows a distribution slightly skewed towards smaller diameters with an average close to 1 cm. Further investigation of the aggregate distribution pattern is needed test if this distribution pattern will be found consistent over larger scale and deeper insight into the cryoconite formation process will be needed for its interpretation.

The presence of seabird nesting sites on the valley walls adjacent to Aldegondabreen suggests a potential for high organic nutrient input into the system (Odasz 1994, Stempniewicz 2005, Ellis *et al* 2006, Zwolicki *et al* 2013), especially at the sides of the glacier. The measured concentrations of both sediment-bound and dissolved nitrogen in our samples were, however, similar to those on other Svalbard glaciers (Stibal *et al* 2008b, Hodson *et al* 2010,

Telling *et al* 2011, Cameron *et al* 2012a, Ansari *et al* 2013). The only exception was ammonium (NH_4^+) which is usually close to detection limit in supraglacial meltwaters (Hodson *et al* 2010, Ansari *et al* 2013) but was detected in significant amounts (5.0–30 $\mu g\, l^{-1}$) in most of our meltwater and surface ice samples. The samples with ammonium below detection limit were A1 supraglacial meltwater and A1 and A2 surface ice in lower part of transect A (figure 1(B)). It is also likely that organic nutrients were additionally supplied to the edges of the glacier from the seabird colonies, as found on other Svalbard glaciers (Stibal *et al* 2008b, Telling *et al* 2011). However, it is probable that unlike many other glaciers, the supply of NH_4^+ to Aldegondabreen is supplemented by local seabird colonies and therefore not heavily dependent on the seasonal process of snow melt like many other glaciers here (Hodson *et al* 2005, Telling *et al* 2011, Ansari *et al* 2013). This is important, because mass balance studies show how supraglacial microbial assimilation of snowmelt-derived NH_4^+ represents one of the most significant processes in the nitrogen cycling of maritime polar ecosystems (Hodson *et al* 2005, Hodson 2006).

The low concentrations of NH_4^+ in some of the supraglacial meltwater samples were associated with significant cryoconite cover and so they might testify to areas where NH_4^+ assimilation outpaced supply during our study. Thereafter, the potential microbial pathways also include nitrification, which has been hypothesized to occur in glacial sediments such as cryoconite (Wynn *et al* 2007, Hodson *et al* 2010, Ansari *et al* 2013), and is thought to result in the well-known surplus of NO_3^- typically observed in glacial runoff from Svalbard glaciers (Hodson *et al* 2005). Ammonia oxidizers use NH_4^+ as a source of energy, oxidizing it to nitrite (Kowalchuk and Stephen 2001), and might therefore constitute a major pathway for the production of the NO_3^- surplus. The *amoA* gene encodes a subunit of ammonia monooxygenase catalysing the first step in ammonia oxidation (McTavish *et al* 1993), and is used as a marker for ammonia oxidizers (Kowalchuk and Stephen 2001). Both bacteria (AOB, Beta- and Gammaproteobacteria) and archaea (AOA, Thaumarchaeota) are known to oxidize ammonia, and AOA have been shown to outnumber AOB in most soil environments (Leininger *et al* 2006). We detected two orders of magnitude higher numbers of archaeal *amoA* compared to bacterial *amoA* in our samples using qPCR, which is consistent with this finding and suggests that cryoconite may be yet another archaea-dominated ammonia oxidation environment. This is further supported by the detection of several sequences of AOA within the Nitrososphaeraceae group (figure 6). It is notable that these sequences were most similar to those from other cold ecosystems, including cryoconite from Antarctica (Cameron *et al* 2012a), Canadian Arctic permafrost (Steven *et al* 2008), and Svalbard top soil (Alves *et al* 2013). Whilst bacterial *amoA* has been detected in cryoconite on Rieperbreen, a Svalbard glacier <50 km from Aldegondabreen (Cameron *et al* 2012b) and in melting snow on Larsbreen adjacent to Longyearbyen (Hell *et al* 2013), this is the first evidence of ammonia-oxidizing archaea present on an Arctic glacier.

Our results suggest that the presence of ammonia oxidizers is principally controlled by the sediment character (figure 4). Therefore, we suggest that the combination of factors contributing to the formation of large cryoconite aggregates present on Aldegondabreen, as mentioned above, enables the functioning of specialized microbial guilds such as ammonia oxidizers in this case. Other metabolic pathways requiring stable conditions otherwise not attainable on the glacier surface may be possible within these large aggregates and should be a focus of future research of biogeochemical processes in glacial ecosystems.

Given the potential importance of sea birds as nutrient vectors in the present study, it is worth considering whether the case of Aldegondabreen represents an exceptional case, or if such bird colonies near glaciers are commonplace in Svalbard. The available data on the distribution of seabird colonies (Norsk Polar Institute, http://svalbardkartet.npolar.no/Viewer.html?Viewer=Svalbardkartet) show at least tens of cases where bird colonies lie above glacial surfaces in Western Svalbard. These glaciers are not in close proximity to the usually visited sites surrounding Ny-Ålesund and Longyearbyen. Therefore, more effort needs to be directed outside of these areas if the role of marine ecosystems in the subsidy of glacial ecosystems is to be fully appreciated.

5. Conclusions

The surface of Aldegondabreen, a small valley glacier in Svalbard, receives carbon and nutrients from multiple sources, including bird nesting sites on the adjacent valley walls. The combination of nutrient input, slope-related supraglacial meltwater flow and the presence of fine surface debris (cryoconite) likely supports the formation of large cryoconite aggregates found in some areas of the glacier surface. A diverse microbial community was found to inhabit the cryoconite on Aldegondabreen, dominated by the cyanobacteria, Proteobacteria, Bacteroidetes, and Actinobacteria, typical for supraglacial environments. Allochthonous material including chloroplasts (probably plant tissue-derived) was also identified in the molecular analysis. Importantly, ammonia-oxidizing archaea (AOA) were, for the first time on an Arctic glacier, detected in the large aggregates, using qPCR targeting the *amoA* gene involved in the first step of ammonia oxidation and pyrosequencing of 16S rRNA genes. The archaea could potentially contribute to the immobilization of NH_4^+ and the production of surplus NO_3^-. More attention should, therefore, be paid to these large aggregates and the potentially important microbial processes occurring in them.

Acknowledgments

This research was supported from Marie-Curie ITN NSINK Project No. 215503. The authors also acknowledge a Royal Geographical Society Peter Fleming Award and a grant from the National Geographic Committee for Research and Exploration to AH which funded the field campaign. Microbiological analysis was supported from Danish Research Council grant FNU 10-085274 to CSJ.

JZ acknowledges a scholarship of the University of Innsbruck (2011/2/Bio22 140797). We thank Reinhard Starnberger, Josef Franzoi, Gry Bjorg Larsen (University of Innsbruck), Pia Bach Jakobsen, Louise Feld (GEUS) and Karin Vestberg (University of Copenhagen) for laboratory assistance, and Harry Langford (University of Sheffield) for field assistance.

References

Alves R J E, Wanek W, Zappe A, Richter A, Svenning M M, Schleper C and Urich T 2013 Nitrification rates in Arctic soils are associated with functionally distinct populations of ammonia-oxidizing archaea *ISME J.* **7** 1620–31

Anesio A M, Sattler B, Foreman C, Telling J, Hodson A, Tranter M and Psenner R 2010 Carbon fluxes through bacterial communities on glacier surfaces *Ann. Glaciol.* **51** 32–40

Ansari A H, Hodson A J, Heaton T H E, Kaiser J and Marca-Bell A 2013 Stable isotopic evidence for nitrification and denitrification in a high Arctic glacial ecosystem *Biogeochemistry* **113** 341–57

Battin T J, Sloan W T, Kjelleberg S, Daims H, Head I M, Curtis T P and Eberl L 2007 Microbial landscapes: new paths to biofilm research *Nature Rev. Microbiol.* **5** 76–81

Björkman M P, Kühnel R, Partridge D G, Roberts T J, Aas W, Mazzola M, Viola A, Hodson A, Ström J and Isaksson E 2013 Nitrate dry deposition in Svalbard *Tellus* B **65** 19071

Bøggild C E, Brandt R E, Brown K J and Warren S G 2010 The ablation zone in northeast Greenland: ice types, albedos and impurities *J. Glaciol.* **56** 101–13

Bullard J E 2013 Contemporary glacigenic inputs to the dust cycle *Earth Surf. Process. Landforms* **38** 71–89

Cameron K A, Hodson A J and Osborn A M 2012a Structure and diversity of bacterial, eukaryotic and archaeal communities in glacial cryoconite holes from the Arctic and the Antarctic *FEMS Microbiol. Ecol.* **82** 254–67

Cameron K A, Hodson A J and Osborn A M 2012b Carbon and nitrogen biogeochemical cycling potentials of supraglacial cryoconite communities *Polar Biol.* **35** 1375–93

Caporaso J G *et al* 2010 QIIME allows analysis of high-throughput community sequencing data *Nature Methods* **7** 335–6

DeSantis T Z, Hugenholtz P, Larsen N, Rojas M, Brodie E L, Keller K, Huber T, Dalevi D, Hu P and Andersen G L 2006 Greengenes, a chimera-checked 16S rRNA gene database and workbench compatible with ARB *Appl. Environ. Microbiol.* **72** 5069–72

Edgar R C 2004 MUSCLE: multiple sequence alignment with high accuracy and high throughput *Nucl. Acids Res.* **32** 1792–7

Edgar R C 2010 Search and clustering orders of magnitude faster than BLAST *Bioinformatics* **26** 2460–1

Edwards A, Anesio A M, Rassner S M, Sattler B, Hubbard B P, Perkins W T, Young M and Griffith G W 2011 Possible interactions between bacterial diversity, microbial activity and supraglacial hydrology of cryoconite holes in Svalbard *ISME J.* **5** 150–60

Edwards A, Rassner S M E, Anesio A M, Worgan H J, Irvine-Fynn T D L, Williams H W, Sattler B and Griffith G W 2013 Contrasts between the cryoconite and ice-marginal bacterial communities of Svalbard glaciers *Polar Res.* **32** 19468

Ellis J C, Farina J M and Whitman J D 2006 Nutrient transfer from sea to land: the case of gulls and cormorants in the Gulf of Maine *J. Anim. Ecol.* **75** 565–74

Gardner A S, Moholdt G, Wouters B, Wolken G J, Burgess D O, Sharp M J, Cogley J G, Braun C and Labine C 2011 Sharply increased mass loss from glaciers and ice caps in the Canadian Arctic Archipelago *Nature* **473** 357–60

Garritano S, Gemignani F, Voegele C, Nguyen-Dumont T, Le Calvez-Kelm F, De Silva D, Lesueur F, Landi S and Tavtigian S V 2009 Determining the effectiveness of high resolution melting analysis for SNP genotyping and mutation scanning at the TP53 locus *BMC Genet.* **10** 5

Hansen C H F, Krych L, Nielsen D S, Vogensen F K, Hansen L H, Sørensen S J, Buschard K and Hansen A K 2012 Early life treatment with vancomycin propagates *Akkermansia muciniphila* and reduces diabetes incidence in the NOD mouse *Diabetologia* **55** 2285–94

Hansen J and Nazarenko L 2003 Soot climate forcing via snow and ice albedos *Proc. Natl Acad. Sci. USA* **101** 423–8

Hell K, Edwards A, Zarsky J, Podmirseg S M, Girdwood S, Pachebat J A, Insam H and Sattler B 2013 The dynamic bacterial communities of a melting High Arctic snowpack *ISME J.* **7** 1814–26

Hodson A 2006 Biogeochemistry of snowmelt in an Antarctic glacial ecosystem *Water Resources Res.* **42** W11406

Hodson A, Anesio A M, Tranter M, Fountain A G, Osborn M, Priscu J, Laybourn-Parry J and Sattler B 2008 Glacial ecosystems *Ecol. Monogr.* **78** 41–67

Hodson A, Cameron K, Bøggild C, Irvine-Fynn T, Langford H, Pearce D and Banwart S 2010 The structure, biological activity and biogeochemistry of cryoconite aggregates upon an Arctic valley glacier: Longyearbreen, Svalbard *J. Glaciol.* **56** 349–61

Hodson A, Roberts T J, Engvall A-C, Holmén K and Mumford P 2009 Glacier ecosystem response to episodic nitrogen enrichment in Svalbard, European high Arctic *Biogeochemistry* **98** 171–84

Hodson A J, Mumford P N, Kohler J and Wynn P M 2005 The high Arctic glacial ecosystem: new insights from nutrient budgets *Biogeochemistry* **72** 233–56

Iizumi T, Mizumoto M and Nakamura K 1998 A bioluminescence assay using *Nitrosomonas europaea* for rapid and sensitive detection of nitrification inhibitors *Appl. Environ. Microbiol.* **64** 3656–62

Irvine-Fynn T D L, Bridge J W and Hodson A J 2011 *In situ* quantification of supraglacial cryoconite morphodynamics using time-lapse imaging: an example from Svalbard *J. Glaciol.* **57** 651–7

Kaštovská K, Stibal M, Šabacká M, Černá B, Šantrůčková H and Elster J 2007 Microbial community structure and ecology of subglacial sediments in two polythermal Svalbard glaciers characterized by the epifluorescence microscopy and PLFA *Polar Biol.* **30** 277–87

Kekonen T, Moore J, Perämäki P, Mulvaney R, Isaksson E, Pohjola V and van de Wal R S W 2005 The 800 year long ion record from the Lomonosovfonna (Svalbard) ice core *J. Geophys. Res.* **110** D07304

Kohler J, James T D, Murray T, Nuth C, Brandt O, Barrand N E, Aas H F and Luckman A 2007 Acceleration in thinning rate on western Svalbard glaciers *Geophys. Res. Lett.* **34** 1944–8007

Kowalchuk G A and Stephen J R 2001 Ammonia-oxidizing bacteria: a model for molecular microbial ecology *Annu. Rev. Microbiol.* **55** 485–529

Kühnel R, Roberts T J, Björkman M P, Isaksson E, Aas W, Holmén K and Ström J 2012 20-year climatology of NO_3^- and NH_4^+ wet deposition at Ny-Ålesund, Svalbard *Adv. Meteorol.* **10** 406508

Langford H, Hodson A and Banwart S 2011 Using FTIR spectroscopy to characterise the soil mineralogy and geochemistry of cryoconite from Aldegondabreen glacier, Svalbard *Appl. Geochem.* **26** 206–9

Langford H, Hodson A, Banwart S and Bøggild C 2010 The microstructure and biogeochemistry of Arctic cryoconite granules *Ann. Glaciol.* **51** 87–94

Leininger S, Urich T, Schloter M, Schwark L, Qi J, Nicol G W, Prosser J I, Schuster S C and Schleper C 2006 Archaea

predominate among ammonia-oxidizing prokaryotes in soils *Nature* **442** 806–9
McConnell J R, Edwards R, Kok G L, Flanner M G, Zender C S, Saltzman E S, Banta J R, Pasteris D R, Carther M M and Kahl J D W 2007 20-century industrial black carbon emissions altered Arctic climate forcing *Science* **317** 1381–4
McTavish H, Fuchs J A and Hooper A B 1993 Sequence of the gene coding for ammonia monooxygenase in *Nitrosomonas europaea J. Bacteriol.* **175** 2436–44
Moholdt G, Nuth C, Hagen J O and Kohler J 2010 Recent elevation changes of Svalbard glaciers derived from ICESat laser altimetry *Remote Sens. Environ.* **114** 2756–67
Muyzer G, de Waal E C and Uitterlinden A G 1993 Profiling of complex microbial populations by denaturing gradient gel electrophoresis analysis of polymerase chain reaction-amplified genes coding for 16S rRNA *Appl. Environ. Microbiol.* **59** 695–700
Navarro F J, Glazovsky A F, Macheret Yu Ya, Vasilenko E V, Corcuera M I and Cuadrado M L 2005 Ice-volume changes (1936–1990) and structure of Aldegondabreen, Spitsbergen *Ann. Glaciol.* **42** 158–62
Nuth C, Moholdt G, Kohler J, Hagen J O and Kääb A 2010 Svalbard glacier elevation changes and contribution to sea level rise *J. Geophys. Res.* **115** F01008
Odasz A M 1994 Nitrate reductase activity in vegetation below an Arctic bird cliff, Svalbard, Norway *J. Veg. Sci.* **5** 913–20
Pritchard H D, Arthern R J, Vaughan D G and Edwards L A 2009 Extensive dynamic thinning on the margins of the Greenland and Antarctic ice sheets *Nature* **461** 971–5
Rotthauwe J-H, Witzel K-P and Liesack W 1997 The ammonia monooxygenase structural gene *amoA* as a functional marker: molecular fine-scale analysis of natural ammonia-oxidizing populations *Appl. Environ. Microbiol.* **63** 4704–12
Samyn D, Vega C P, Motoyama H and Pohjola V A 2012 Nitrate and sulfate anthropogenic trends in the 20th century from five Svalbard ice cores *Arct. Antarct. Alp. Res.* **44** 490–9
Schauss K *et al* 2009 Dynamics and functional relevance of ammonia-oxidizing archaea in two agricultural soils *Environ. Microbiol.* **11** 446–56
Slater J F, Currie L A, Dibb J E and Benner B A Jr 2002 Distinguishing the relative contribution of fossil fuel and biomass combustion aerosols deposited at Summit, Greenland through isotopic and molecular characterization of insoluble carbon *Atmos. Environ.* **36** 4463–77
Sperazza M, Moore J N and Hendrix M S 2004 High-resolution particle size analysis of naturally occuring very fine-grained sediment trough laser diffractometry *J. Sediment. Res.* **74** 736–43
Stempniewicz L 2005 Keystone species and ecosystem functioning. Seabirds in polar ecosystems *Ecol. Questions* **6** 111–5
Steven B, Pollard W H, Greer C W and Whyte L G 2008 Microbial diversity and activity through a permafrost/ground ice core profile from the Canadian high Arctic *Environ. Microbiol.* **10** 3388–403
Stibal M, Šabacká M and Žárský J 2012a Biological processes on glacier and ice sheet surfaces *Nature Geosci.* **5** 771–4
Stibal M, Telling J, Cook J, Mak K M, Hodson A and Anesio A M 2012b Environmental controls on microbial abundance and activity on the Greenland ice sheet: a multivariate analysis approach *Microb. Ecol.* **63** 74–84
Stibal M, Tranter M, Benning L G and Řehák J 2008a Microbial primary production on an Arctic glacier is insignificant in comparison with allochthonous organic carbon input *Environ. Microbiol.* **10** 2172–8
Stibal M, Tranter M, Telling J and Benning L G 2008b Speciation, phase association and potential bioavailability of phosphorus on a Svalbard glacier *Biogeochemistry* **90** 1–13
Takeuchi N, Kohshima S and Seko K 2001 Structure, formation, and darkening process of albedo-reducing material (cryoconite) on a Himalayan glacier: a granular algal mat growing on the glacier *Arct. Antarct. Alp. Res.* **33** 115–22
Takeuchi N, Nishiyama H and Li Z Q 2010 Structure and formation process of cryoconite granules on Urumqi glacier No. 1, Tien Shan, China *Ann. Glaciol.* **51** 9–14
Tamura K, Peterson D, Peterson N, Stecher G, Nei M and Kumar S 2011 MEGA5: molecular evolutionary genetics analysis using maximum likelihood, evolutionary distance, and maximum parsimony methods *Mol. Biol. Evol.* **28** 2731–9
Telling J, Anesio A M, Tranter M, Irvine-Fynn T, Hodson A, Butler C and Wadham J 2011 Nitrogen fixation on Arctic glaciers, Svalbard *J. Geophys. Res.* **116** G03039
ter Braak C J F and Šmilauer P 2012 *Canoco Reference Manual and User's Guide: Software for Ordination (Version 5.0)* (Ithaca, NY: Microcomputer Power) p 496
Treusch A H, Leininger S, Kietzin A, Schuster S C, Klenk H-P and Schleper C 2005 Novel genes for nitrite reductase and Amo-related proteins indicate a role of uncultivated mesophilic Crenarchaeota in nitrogen cycling *Environ. Microbiol.* **7** 1985–95
Vogler P 1966 Zur Analytik der Phosphorverbindungen in Gewässern *Limnologica* **4** 437–44
Wang Q, Garrity G M, Tiedje J M and Cole J R 2007 Naive Bayesian classifier for rapid assignment of rRNA sequences into the new bacterial taxonomy *Appl. Environ. Microbiol.* **73** 5261–7
Waterhouse A M, Procter J B, Martin D M A, Clamp M and Barton G J 2009 Jalview version 2—a multiple sequence alignment editor and analysis workbench *Bioinformatics* **25** 1189–91
Wynn P M, Hodson A J, Heaton T H E and Chenery S R 2007 Nitrate production beneath a high Arctic glacier, Svalbard *Chem. Geol.* **244** 88–102
Zmudczyńska K, Zwolicki A, Barcikowski M, Iliszko L and Stempniewicz L 2008 Variability of individual biomass and leaf size of *Saxifraga nivalis* L. along a transect between seabirds colony and seashore in Hornsund, Spitsbergen *Ecol. Questions* **9** 37–44
Zwolicki A, Zmudczynska-Skarbek K M, Iliszko L and Stempniewicz L 2013 Guano deposition and nutrient enrichment in the vicinity of planktivorous and piscivorous seabird colonies in Spitsbergen *Polar Biol.* **36** 363–72